# Spectroscopy of the neutron-rich hypernucleus HeΛ7 from electron scattering

(HKS(JLab E05-115) Collaboration) Gogami, T.; ...; Androić, Darko; ...; Furić, Miroslav; ...; Petković, Tomislav; ...; Ševa, Tomislav; ...; ...

# Spectroscopy of the neutron-rich hypernucleus $^{7}_{\Lambda}$He from electron scattering

T. Gogami,[1,*] C. Chen,[2] D. Kawama,[1] P. Achenbach,[3] A. Ahmidouch,[4] I. Albayrak,[2] D. Androic,[5] A. Asaturyan,[6] R. Asaturyan,[6,†] O. Ates,[2] P. Baturin,[7] R. Badui,[7] W. Boeglin,[7] J. Bono,[7] E. Brash,[8] P. Carter,[8] A. Chiba,[1] E. Christy,[2] S. Danagoulian,[4] R. De Leo,[9] D. Doi,[1] M. Elaasar,[10] R. Ent,[11] Y. Fujii,[1] M. Fujita,[1] M. Furic,[5] M. Gabrielyan,[7] L. Gan,[12] F. Garibaldi,[13] D. Gaskell,[11] A. Gasparian,[4] Y. Han,[2] O. Hashimoto,[1,†] T. Horn,[11] B. Hu,[14] Ed. V. Hungerford,[15] M. Jones,[11] H. Kanda,[1] M. Kaneta,[1] S. Kato,[16] M. Kawai,[1] H. Khanal,[17] M. Kohl,[2] A. Liyanage,[2] W. Luo,[14] K. Maeda,[1] A. Margaryan,[6] P. Markowitz,[7] T. Maruta,[1] A. Matsumura,[1] V. Maxwell,[7] A. Mkrtchyan,[6] H. Mkrtchyan,[6] S. Nagao,[1] S. N. Nakamura,[1] A. Narayan,[17] C. Neville,[7] G. Niculescu,[18] M. I. Niculescu,[18] A. Nunez,[7] Nuruzzaman,[17] Y. Okayasu,[1] T. Petkovic,[5] J. Pochodzalla,[3] X. Qiu,[14] J. Reinhold,[7] V. M. Rodriguez,[19] C. Samanta,[20] B. Sawatzky,[11] T. Seva,[5] A. Shichijo,[1] V. Tadevosyan,[6] L. Tang,[2,11] N. Taniya,[1] K. Tsukada,[1] M. Veilleux,[8] W. Vulcan,[11] F. R. Wesselmann,[21] S. A. Wood,[11] T. Yamamoto,[1] L. Ya,[2] Z. Ye,[2] K. Yokota,[1] L. Yuan,[2] S. Zhamkochyan,[6] and L. Zhu[2]

(HKS (JLab E05-115) Collaboration)

[1]*Graduate School of Science, Tohoku University, Sendai, Miyagi 980-8578, Japan*
[2]*Department of Physics, Hampton University, Hampton, Virginia 23668, USA*
[3]*Institute for Nuclear Physics, Johannes Gutenberg-University, D-55099 Mainz, Germany*
[4]*Department of Physics, North Carolina A&T State University, Greensboro, North Carolina 27411, USA*
[5]*Department of Physics and Department of Applied Physics, University of Zagreb, HR-10000 Zagreb, Croatia*
[6]*A.I. Alikhanyan National Science Laboratory, Yerevan 0036, Armenia*
[7]*Department of Physics, Florida International University, Miami, Florida 27411, USA*
[8]*Department of Physics, Computer Science & Engineering, Christopher Newport University, Newport News, Virginia 23606, USA*
[9]*Istituto Nazionale di Fisica Nucleare, Sezione di Bari, University of Bari, I-70126 Bari, Italy*
[10]*Department of Physics, Southern University at New Orleans, New Orleans, Lousiana 70126, USA*
[11]*Thomas Jefferson National Accelerator Facility (JLab), Newport News, Virginia 23606, USA*
[12]*Department of Physics, University of North Carolina Wilmington, Wilmington, North Carolina 28403, USA*
[13]*INFN, Sezione Sanità, Istituto Superiore di Sanità, 00161 Rome, Italy*
[14]*Nuclear Physics Institute, Lanzhou University, Gansu 730000, China*
[15]*Department of Physics, University of Houston, Houston, Texas 77204, USA*
[16]*Department of Physics, Yamagata University, Yamagata 990-8560, Japan*
[17]*Mississippi State University, Mississippi State, Mississippi 39762, USA*
[18]*Department of Physics and Astronomy, James Madison University, Harrisonburg, Virginia 22807, USA*
[19]*Escuela de Ciencias y Tecnologia, Universidad Metropolitana, San Juan 00928, Puerto Rico*
[20]*Department of Physics & Astronomy, Virginia Military Institute, Lexington, Virginia 24450, USA*
[21]*Department of Physics, Xavier University of Louisiana, New Orleans, Louisiana 70125, USA*

The missing mass spectroscopy of the $^{7}_{\Lambda}$He hypernucleus was performed using the $^{7}$Li$(e,e'K^{+})^{7}_{\Lambda}$He reaction at the Thomas Jefferson National Accelerator Facility Hall C. The $\Lambda$-binding energy of the ground-state $(1/2^{+})$ was determined with a smaller error than that of the previous measurement, being $B_{\Lambda} = 5.55 \pm 0.10^{\text{stat.}} \pm 0.11^{\text{sys.}}$ MeV. The experiment also provided new insight into charge symmetry breaking in $p$-shell hypernuclear systems. Finally, a peak at $B_{\Lambda} = 3.65 \pm 0.20^{\text{stat.}} \pm 0.11^{\text{sys.}}$ MeV was observed and assigned as a mixture of $3/2^{+}$ and $5/2^{+}$ states, confirming the "gluelike" behavior of $\Lambda$, which makes an unstable state in $^{6}$He stable against neutron emission.

Nuclear physicists explore the low-energy behavior of the strongly interacting many-body systems, extracting an effective potential which can be used for nuclear structure and interaction calculations. Effective potential techniques can also be applied to hypernuclear systems as the lifetime of a hyperon in a nucleus is much greater than the relaxation time associated with strong interactions. On the other hand, the two-body potentials for the hyperon-nucleon interaction $YN$ are not determined as well as those for $NN$ due to the experimental difficulties of producing and detecting hyperons in free scattering experiments. However, embedding a hyperon within the nuclear medium (hypernucleus) does allow extraction of effective potentials from detailed measurements of hypernuclear energy levels and transitions.

Although many species of $\Lambda$ hypernuclei with masses $A \leqslant 209$ have been observed [1,2], more systematic and precise data are still needed for further insight into the $\Lambda N$ interaction. Nowadays, experimental studies of $\Lambda$ hypernuclei use: (1) hadron beams at the Japan Proton Accelerator

---

*Current address: Research Center for Nuclear Physics, Osaka University, Ibaraki, Osaka 567-0047, Japan.

†Deceased.

Research Complex (J-PARC) [3,4], (2) heavy-ion beams at GSI [5–7], (3) heavy-ion colliders at the Brookhaven National Laboratory Relativistic Heavy Ion Collider [8] and the CERN Large Hadron Collider [9], and (4) electron beams at the Mainz Microtron [10,11] and the Thomas Jefferson National Accelerator Facility (JLab) [12–21]. The different production mechanisms are complementary and allow us to use their specific sensitivities to excite particular structures which highlight nuclear features of interest.

One such feature of interest is charge symmetry breaking (CSB) in $\Lambda$ hypernuclei. The difference in ground-state binding energies in the $A = 3$ nonstrange nuclei ($^3$He and $^3$H) is $0.7638 \pm 0.0003$ MeV [22]. There remains a binding-energy difference of 0.081 MeV after accounting for the 0.683-MeV Coulomb correction [23]. In $s$-shell hypernuclei, a large CSB $\Delta B_\Lambda(^4_\Lambda\text{He} - ^4_\Lambda\text{H}; 0^+) = B_\Lambda(^4_\Lambda\text{He}; 0^+) - B_\Lambda(^4_\Lambda\text{H}; 0^+) = (2.39 \pm 0.03) - (2.04 \pm 0.04) = +0.35 \pm 0.06$ MeV is found by comparing the ground-state binding energies between $^4_\Lambda$H and $^4_\Lambda$He [24]. Although the Coulomb effect of the core nuclei $^3$He and $^3$H is already subtracted in the $\Delta B_\Lambda(^4_\Lambda\text{He} - ^4_\Lambda\text{H}; 0^+)$ calculation, the binding-energy difference of the above hypernuclear isospin doublet is due, in part, to differences in the Coulomb energy caused by contraction of the nucleus as a result of the additional $\Lambda$ binding. The Coulomb-energy correction was predicted as $\Delta B_C = 0.02$–0.08 MeV [25–27], and thus $\Delta B_\Lambda(^4_\Lambda\text{He} - ^4_\Lambda\text{H}; 0^+) + \Delta B_C \simeq 0.4$ MeV is attributed to the $\Lambda N$ CSB for the $0^+$ state in the $A = 4$ isodoublet hypernuclear system. This difference in the binding energy is approximately five times larger than for $A = 3$ nonstrange nuclei. A recent $\gamma$-ray measurement indicates that little binding-energy difference exists between the $(1^+)$ exited states [4] although it was believed that the $1^+$ excited states had as large CSBs as the ground states [28–30]. These residual differences are difficult to explain by Coulomb energy alone. A detailed discussion of hypernuclear CSB [31–33] in addition to other topics of interest have been recently published [34].

CSB in $p$-shell hypernuclear systems is predicted to be smaller than in $s$-shell systems [31]. Hence, differences in $\Lambda$-binding energies between $p$-shell mirror hypernuclei are predicted to be less than a few 100 keV [31]. Previous experiments at JLab Hall C measured $\Lambda$-binding energies of $^7_\Lambda$He [18], $^9_\Lambda$Li [35], $^{10}_\Lambda$Be [21], $^{12}_\Lambda$B [12,13,19], $^{28}_\Lambda$Al [16], and $^{52}_\Lambda$V [35] via the $(e,e'K^+)$ reaction. The present Rapid Communication reports a new result for the $\Lambda$-binding energy of $^7_\Lambda$He with an improved systematic error and is compared to its isotopic mirror hypernuclei. In addition, due to improved statistics, the experiment extracted the first observation of a peak corresponding to the excited states $(3/2^+, 5/2^+)$ of $^7_\Lambda$He.

CSB in hypernuclear $p$-shell systems can be studied by comparing the $\Lambda$-binding energies for $A = 7$, isotriplet ($T = 1$) $\Lambda$ hypernuclei, which are the simplest $p$-shell hypernuclear systems $^7_\Lambda$He ($\alpha + n + n + \Lambda$), $^7_\Lambda$Li$^*$ ($\alpha + p + n + \Lambda$), and $^7_\Lambda$Be ($\alpha + p + p + \Lambda$). The isospin of the ground state of $^7_\Lambda$Li is $T = 0$. Thus, an excited state of $^7_\Lambda$Li with $T = 1$ should be compared with the isotriplet partners. The ground-state binding energies of $^7_\Lambda$Li ($T = 0$) and $^7_\Lambda$Be were measured to be $5.58 \pm 0.03$ and $5.16 \pm 0.08$ MeV, respectively, by the emulsion experiments [36]. The binding energy of $^7_\Lambda$Li$^*$ ($T =$

1) is obtained as $5.26 \pm 0.03$ MeV by using information of the energy spacing of $E_x(^7_\Lambda\text{Li}^*; T = 1, 1/2^+) = 3.88$ MeV measured by the $\gamma$-ray spectroscopy [37] and the excitation energy of $E_x(^6\text{Li}^*; T = 1) = 3.56$ MeV [38]. The ground state $(1/2^+)$ $\Lambda$-binding energy of $^7_\Lambda$He using the $(e,e'K^+)$ reaction at JLab Hall C (JLab E01-011) was successfully determined to be $B_\Lambda = 5.68 \pm 0.03^\text{stat.} \pm 0.25^\text{sys.}$ MeV [18]. As a result, the measured energies of $A = 7$, $T = 1$ hypernuclei differ from a cluster model prediction which used a phenomenological $\Lambda N$ CSB potential which was constructed to reproduce the energies of $^4_\Lambda$He and $^4_\Lambda$H [39]. The error on the $\Lambda$-binding energy of $^7_\Lambda$He was larger than for other $\Lambda$ hypernuclei and was dominated by systematic contributions. Therefore the present experiment (JLab E05-115) focused on the determination of the $\Lambda$-binding energy of $^7_\Lambda$He with particular emphasis on reducing the systematic error.

The core nucleus $^6$He ($\alpha + n + n$) in $^7_\Lambda$He is known as a typical neutron-halo nucleus. The first excited-state energy of $^6$He $(2^+)$ was measured to be 0.824 MeV above the $\alpha + n + n$ breakup threshold, having a decay width of $\Gamma = 0.113$ MeV [38]. The corresponding states of $^7_\Lambda$He $(3/2^+, 5/2^+)$ in which $\Lambda$ resides in the $s$ orbit are predicted to be stable against neutron-emission breakup [39–41] due to the attractive $\Lambda N$ interaction. In addition, the existence of isomeric states in $^7_\Lambda$He [42–44] was speculated from widely scattered binding energy obtained by the emulsion experiment, although it had not been confirmed yet experimentally. The production cross section for a sum of these states $(3/2^+, 5/2^+)$ with the $(\gamma, K^+)$ reaction at the small $K^+$ scattering angle was predicted to be $\approx 60\%$ of that for the ground state $(1/2^+)$ [40]. Although a small structure was observed in the spectrum which might correspond to the $3/2^+$ and $5/2^+$ states, a lack of statistics prevented confirmation of the observation of these states in the previous measurement [18]. The present experiment acquired five times higher statistics and can now confirm observation of these states and thus the "gluelike" behavior of $\Lambda$. This Rapid Communication reports the observation of the ground state $(1/2^+)$, and for the first time, the observation of the $3/2^+$ and $5/2^+$ states.

The $(e,e'K^+)$ reaction was used for $\Lambda$ hypernuclear production. Electroproduction is related to photoproduction through a virtual photon produced in the $(e,e')$ reaction [45–47]. In the geometry for JLab E05-115, the virtual photon can be treated as almost real since the square of the four-momentum transfer $Q^2(= -q^2 > 0)$ is quite small [$Q^2 \simeq 0.01$ (GeV/$c$)$^2$]. The experimental kinematics can be found in Ref. [19]. We used a continuous-wave electron beam with an energy of $E_e = 2.344$ GeV, provided by the Continuous Electron Beam Accelerator Facility at JLab. The electron beam was transported to the experimental target which was installed at the entrance of a charge separation dipole magnet [splitter magnet (SPL)]. The $K^+$ s ($p^\text{center}_{K^+} = 1.200$ GeV/$c$) and scattered electrons ($p^\text{center}_{e'} = 0.844$ GeV/$c$) were bent in opposite directions by the SPL and were analyzed with a high-resolution kaon spectrometer (HKS) [48,49] and a high-resolution electron spectrometer (HES), respectively. Details for the experimental setup are described in Refs. [19,21,48]. One important feature of the present experiment is the excellent resolution of $\Delta p/p \simeq 2 \times 10^{-4}$ (FWHM) for both $K^+$ and $e'$

at approximately 1 GeV/$c$ due to the optics of the SPL +HKS +HES system. Thus, an energy resolution of about 0.5 MeV (FWHM) was obtained for hypernuclear spectroscopy [19,21].

The positions and angles of the $K^+$ s and scattered electrons at reference planes in the magnetic spectrometers were measured by particle detectors. This information was converted to momentum vectors at the target position with backward transfer matrices (BTMs) representing the optical systems for the SPL + HES and SPL + HKS, respectively, in order to reconstruct the missing mass ($M_{HYP}$). Once the missing mass was obtained, the $\Lambda$-binding energy ($B_\Lambda$) was calculated as $B_\Lambda(^A_\Lambda Z) = M(^{A-1}Z) + M_\Lambda - M_{HYP}(^A_\Lambda Z)$, where $Z$ denotes the proton number and $M(^{A-1}Z)$ and $M_\Lambda$ are the masses of a core nucleus and $\Lambda$.

The energy scale calibration was performed by optimizing the BTMs of the magnetic spectrometer systems [19]. The BTM optimization is also correlated with energy resolution in the resulting hypernuclear spectra. For the BTM optimization, events of $\Lambda$ and $\Sigma^0$ production from the 0.45-g/cm$^2$ polyethylene target were used along with events from the production of the $^{12}_\Lambda$B ground state from a 0.0875-g/cm$^2$ natural carbon target. Systematic errors, which originated from the BTM optimization process, needed to be estimated carefully since the BTM optimization mainly determines the accuracy of the binding energy ($B_\Lambda$) and excitation energy ($E_\Lambda$) of a $\Lambda$ hypernucleus. In order to estimate the achievable energy accuracy, a fully modeled Monte Carlo simulation was performed. As a result, it was found that $B_\Lambda$ and $E_\Lambda$ could be determined with accuracies of $< 0.09$ and $< 0.05$ MeV, respectively, by this optimization method. Another major contribution to the uncertainty on the binding energy is due to energy-loss corrections for the particles in the target. This contribution was also estimated by the Monte Carlo simulation taking into account the target thickness uncertainty. Finally, the total systematic errors for $B_\Lambda$ and $E_\Lambda$ were estimated as 0.11 and 0.05 MeV, respectively [19,21].

An enriched $^7$Li target (purity of 99%) with a thickness of 0.208 g/cm$^2$ was used for the $^7_\Lambda$He production. The nominal beam current for the production run of $^7_\Lambda$He was 35 $\mu$A, and the total incident charge on the $^7$Li target was 4.839 C ($\simeq 3 \times 10^{19}$ electrons). Figure 1 shows the obtained binding energy ($-B_\Lambda$) spectrum with an ordinate axis of $\overline{(\frac{d\sigma}{d\Omega_K})}$ as defined in Ref. [21]. For the binding-energy calculation, the nuclear masses of $M(^7\text{Li}) = 5605.54$ and $M(^6\text{He}) = 6533.83$ MeV [50] were used. Events from quasifree $\Lambda$ production were distributed in the region of $-B_\Lambda > 0$. The distribution of the accidental $e'K^+$-coincidence events in the spectrum was obtained by the mixed events analysis [18]. This method provides an accidental coincidence spectrum with high statistics thus reducing the statistical uncertainty caused by background subtraction.

Figure 2 shows the spectrum of the $\Lambda$-binding energy ($-B_\Lambda$) and the excitation energy $\{E_\Lambda \equiv -[B_\Lambda - B_\Lambda(\#1)]\}$ of $^7_\Lambda$He after the accidental $e'K^+$-coincidence distribution was subtracted. In order to find peak candidates, a peak search by tests of statistical significance defined as $S/\sqrt{S+N}$ was applied. The statistical significance was calculated for each bin of the histogram, and the tests for robustness used several settings of bin size to find peak candidates, taking into account
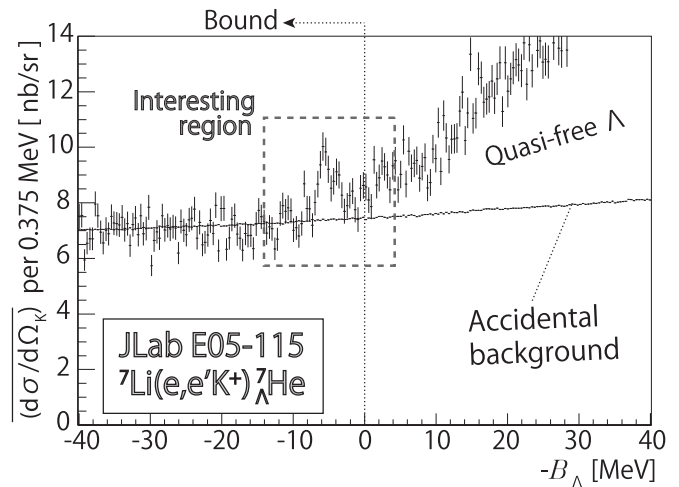


FIG. 1. The binding energy ($-B_\Lambda$) spectrum of $^7_\Lambda$He with an ordinate axis of $\overline{(\frac{d\sigma}{d\Omega_K})}$ defined in Ref. [21].

the energy resolution. As a result, two peak candidates were found with peak separations of $\geqslant 3\sigma$ as labeled by #1 and #2 in Fig. 2. The statistical significance for peak #1 is $7.5\sigma$ in a range of $-7.0$ to $-4.0$ MeV, which is larger than that of the previous measurement ($5.5\sigma$) [18]. The two peak candidates were fitted by Voigt functions (convolution of Gaussian and Lorentzian functions) to obtain $B_\Lambda(E_\Lambda)$ and the differential cross section for each peak. The fitting results are given in Table I. The energy resolution was obtained to be 1.3 MeV (FWHM), which is consistent with the estimation by the Monte Carlo simulation, although our previously published result for $^{12}_\Lambda$B [19] was better (FWHM $\simeq 0.54$ MeV). In the Monte Carlo simulation, it was found that our BTMs have a momentum
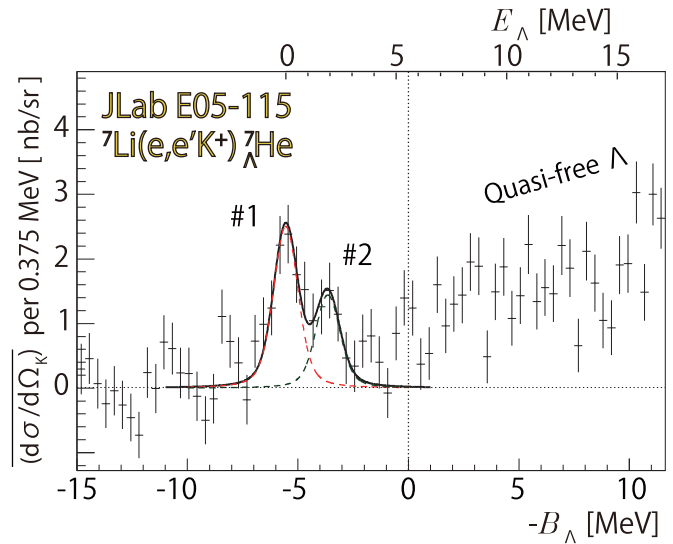


FIG. 2. The spectrum of the binding energy ($-B_\Lambda$) and the excitation energy $\{E_\Lambda \equiv -[B_\Lambda - B_\Lambda(\#1)]\}$ for the $^7\text{Li}(e,e'K^+)^7_\Lambda$He reaction with an ordinate axis of $\overline{(\frac{d\sigma}{d\Omega_K})}$ after the accidental $e'K^+$-coincidence distribution was subtracted. The curve is a fit with two Voigt functions.

TABLE I. Fitting results for the $\Lambda$-binding energy, excitation energy ($E_\Lambda$), and $\overline{(\frac{d\sigma}{d\Omega_K})}$ defined in Ref. [21] for $^7\text{Li}(e,e'K^+)^7_\Lambda\text{He}$. Errors are statistical and systematic.

| Peak | Number of events | $B_\Lambda$ (MeV) [$E_\Lambda$ (MeV)] | $\overline{(\frac{d\sigma}{d\Omega_K})}$ (nb/sr) |
|---|---|---|---|
| #1 | $413 \pm 38$ | $5.55 \pm 0.10 \pm 0.11$ (0.0) | $10.7 \pm 1.0 \pm 1.8$ |
| #2 | $239 \pm 22$ | $3.65 \pm 0.20 \pm 0.11$ ($1.90 \pm 0.22 \pm 0.05$) | $6.2 \pm 0.6 \pm 1.1$ |

dependence on the $z$ displacement (beam direction) from the interaction point. This dependence significantly contributes to the energy resolution, adding a kinematical contribution due to the large recoil of the light hypernuclear system. The length in the $z$ direction of the $^7\text{Li}$ target (4.0 mm) was longer than that of the natural $^{12}\text{C}$ target (0.5 mm) used for a measurement of $^{12}\text{C}(e,e'K^+)^{12}_\Lambda\text{B}$ [19]. Thus, the peak width for $^7_\Lambda\text{He}$ increased with respect to the $^{12}_\Lambda\text{B}$ result as the simulation indicated.

Peak #1 is considered as the ground state of $^7_\Lambda\text{He}$ ($^6\text{He}[J_C; E_x] \otimes j^\Lambda = [0^+; \text{g.s.}] \otimes s^\Lambda_{1/2} = 1/2^+$). The $\Lambda$-binding energy of the $1/2^+$ state was obtained to be $5.55 \pm 0.10^{\text{stat.}} \pm 0.11^{\text{sys.}}$ MeV, which is consistent with the previous result ($5.68 \pm 0.03^{\text{stat.}} \pm 0.25^{\text{sys.}}$ MeV) [18] but with improved uncertainty. For the previous results, the statistical error is smaller since the energy resolution for the $^7_\Lambda\text{He}$ spectrum is better whereas the systematic error dominates. In the present result, on the other hand, statistical and systematic errors are balanced, reducing the total uncertainty by optimizing the target thickness and the energy-calibration method.

Figure 3 shows the measured $\Lambda$-binding energies of $A = 7$, $T = 1$ hypernuclei with statistical error bars as compared
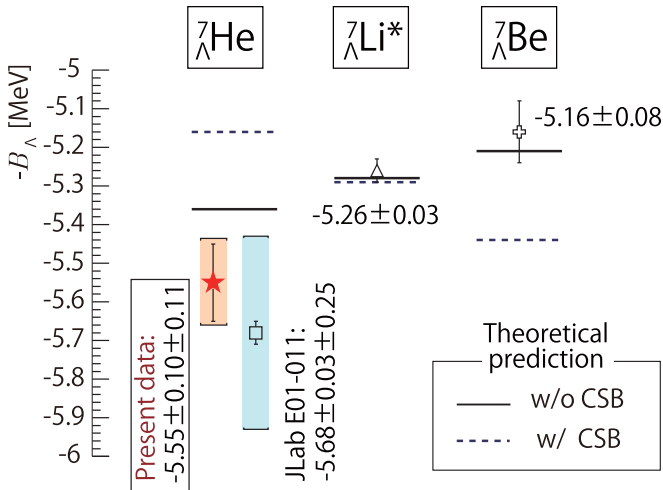
to a theoretical prediction by a four-body cluster model [39]. Colored boxes on the results of $^7_\Lambda\text{He}$ indicate systematic errors on $B_\Lambda$. In the cluster model prediction [39], a phenomenological even-state CSB potential was introduced to reproduce the binding energies of $^4_\Lambda\text{He}$ and $^4_\Lambda\text{H}$. This was applied to the $A = 7$, $T = 1$ hypernuclear system. Binding-energy predictions without and with the phenomenological CSB potential are shown by solid and dashed lines, respectively, in Fig. 3. The present result seems to favor the energy prediction without the phenomenological CSB potential. This is also the case for the other experimental data in the $A = 7$, $T = 1$ system. This comparison suggests that a phenomenological CSB potential needs further consideration. It is possible to introduce a strong odd-state CSB potential in addition to one for the even state in order to make the experiment and theoretical prediction more consistent [39,51], although the validity of a strong odd-state interaction can be questioned [52]. It was suggested that the CSB interaction needs inclusion of explicit $\Lambda N$-$\Sigma N$ coupling [31]. It seems clear that further systematic studies with more precise data particularly for the $p$-shell hypernuclei are needed.

Peak #2 was obtained at $B_\Lambda(\#2) = 3.65 \pm 0.20^{\text{stat.}} \pm 0.11^{\text{sys.}}$ MeV with a differential cross section of $6.2 \pm 0.6^{\text{stat.}} \pm 1.1^{\text{sys.}}$ nb/sr. Figure 4 shows a $B_\Lambda$ comparison between the obtained results and the theoretical predictions [40,41] with energy levels of the core nucleus $^6\text{He}$ [38]. Energy levels of the first excited doublet ($3/2^+, 5/2^+$) are predicted to be approximately 1.7 MeV above the ground-state ($1/2^+$) [40,41]. Moreover, a ratio of the differential cross section of a sum of $3/2^+$ and $5/2^+$ states to that of the ground-state ($1/2^+$) is predicted to be approximately 0.6. The value of $E_\Lambda$ and the ratio of $\overline{(\frac{d\sigma}{d\Omega_K})}$ for peak #1 to peak #2 are $E_\Lambda = 1.90 \pm 0.20^{\text{stat.}} \pm 0.11^{\text{sys.}}$ MeV and $\simeq 0.58$, respectively. The results are consistent with the above theoretical predictions, and thus, peak #2 is interpreted as

$$^6\text{He}[J_C; E_x] \otimes j^\Lambda = [2^+; 1.8 \text{ MeV}] \otimes s^\Lambda_{1/2}$$
$$= (3/2^+, 5/2^+).$$

FIG. 3. Measured $\Lambda$-binding energies of $^7_\Lambda\text{He}$ (present result and Ref. [18]), $^7_\Lambda\text{Li}^*$ [36,37], and $^7_\Lambda\text{Be}$ [36] for the $1/2^+$ state with statistical error bars. Colored boxes on the experimental results of $^7_\Lambda\text{He}$ indicate systematic errors on $B_\Lambda$. The solid and dashed lines represent theoretical calculations without and with a phenomenological even-state $\Lambda N$ CSB potential, which reproduces $\Lambda$-binding energies of $^4_\Lambda\text{He}$ and $^4_\Lambda\text{H}$ by a four-body cluster model [39].
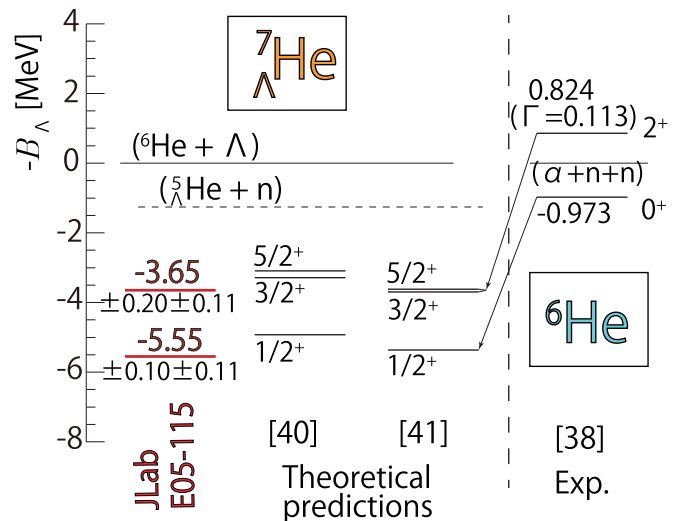
FIG. 4. Obtained energy levels of $^7_\Lambda\text{He}$ with theoretical predictions [40,41]. Reported energy levels for $^6\text{He}$ are also shown [38].

The $3/2^+$ and $5/2^+$ states of $^7_\Lambda$He are more than 2.3 MeV below the $^5_\Lambda$He + $n$ breakup energy [36,38], which is the lowest neutron emission breakup, as shown in Fig. 4. On the other hand, the $2^+$ state of $^6$He, which corresponds to the $3/2^+$ and $5/2^+$ states of $^7_\Lambda$He, was reported to be 0.824 MeV above the $\alpha + n + n$ energy [38] ($E = 1.797 \pm 0.025$ MeV), meaning that this state is not stable against neutron emission. Therefore, the present result of the peak for the $3/2^+$ and $5/2^+$ states in $^7_\Lambda$He confirms the $\Lambda$ gluelike role, making an unbound nucleus bound.

The successful observation of the first excited doublet in $^7_\Lambda$He opens a door to study unstable states of light nuclei. For instance, energy-level predictions of the second $2^+$ state ($2_2^+$) in a neutron-halo nucleus $^6$He are largely different depending on models as shown in Ref. [53]. Recently the excitation energy of a $2_2^+$ state of $^6$He was measured to be $E_x = 2.6 \pm 0.3$ MeV with a width of $\Gamma = 1.6 \pm 0.4$ MeV by the two-neutron transfer reaction $p(^8$He$,t)^6$He [53]. This measurement would exclude several theoretical models. However, the $2_2^+$ energy was derived from a spectral decomposition by fitting to a spectrum in which a few of major states are overlapping because of their large decay widths ($\Gamma =$ a few MeV).

On the other hand, the $3/2_2^+$ and $5/2_2^+$ states in $^7_\Lambda$He, which correspond to the $2_2^+$ state in $^6$He, are predicted to be much narrower [41] due to the additional binding of $\Lambda$. Therefore, a measurement of the $3/2_2^+$ and $5/2_2^+$ states in $^7_\Lambda$He combined with a realistic cluster calculation may provide a better understanding of the $2_2^+$ state in $^6$He. The differential cross section of the sum of the $3/2_2^+$ and $5/2_2^+$ states in $^7_\Lambda$He is predicted to be approximately 16% of that for the ground state [41]. Consequently, the observation of the $3/2_2^+$ and $5/2_2^+$ states in $^7_\Lambda$He is promising for future spectroscopy at JLab using the $(e,e'K^+)$ reaction.

To summarize, the spectroscopy of $\Lambda$ hypernuclei was performed with a new magnetic spectrometer system SPL + HKS + HES at JLab Hall C via the $(e,e'K^+)$ reaction. A spectroscopic measurement of a neutron-rich hypernucleus $^7_\Lambda$He was performed with an enriched $^7$Li target, and the hypernuclear structure was successfully observed with an energy resolution of 1.3-MeV FWHM.

The ground-state energy ($1/2^+$) of $^7_\Lambda$He was determined to be $B_\Lambda = 5.55 \pm 0.10^{\text{stat.}} \pm 0.11^{\text{sys.}}$ MeV, which was consistent with the result of the previous measurement and improved the total error. The $\Lambda$-binding energy provides insight into CSB effects of the $\Lambda N$ interaction by comparison with the bindings of isotopic mirror hypernuclei in the $A = 7$, $T = 1$ system ($^7_\Lambda$Li$^*$, $^7_\Lambda$Be). Further systematic investigations with better precision, particularly for $p$-shell hypernuclei, are necessary in order to deepen our understanding of $\Lambda N$ CSB. The $(e,e'K^+)$ reaction at JLab provides a unique method to measure the absolute $\Lambda$-binding energies of $p$-shell hypernuclei or heavier with less than a few 100-keV accuracy.

The first excited doublet ($3/2^+,5/2^+$) in $^7_\Lambda$He, which corresponds to the $2^+$ state in $^6$He, was successfully observed for the first time. A peak for a sum of the $3/2^+$ and $5/2^+$ was determined to be $B_\Lambda = 3.65 \pm 0.20^{\text{stat.}} \pm 0.11^{\text{sys.}}$ MeV with the differential cross section of $(\frac{d\sigma}{d\Omega_K}) = 6.2 \pm 0.6^{\text{stat.}} \pm 1.1^{\text{sys.}}$ nb/sr. The peak for the $3/2^+$ and $5/2^+$ states was found to be approximately 2.3 MeV below the lowest neutron-emission energy. The result shows that the $2^+$ state in $^6$He, which is an unstable state for the $\alpha + n + n$ breakup, becomes stable against neutron-emission breakup once $\Lambda$ is bound in the nucleus, owing to the additional binding of $\Lambda$.

[1] O. Hashimoto and H. Tamura, Prog. Part. Nucl. Phys. **57**, 564 (2006).

[2] A. Feliciello and T. Nagae, Rep. Prog. Phys. **78**, 096301 (2015).

[3] List of proposed experiments [http://j-parc.jp/researcher/Hadron/en/Experiments_e.html].

[4] T. O. Yamamoto *et al.* (J-PARC E13 Collaboration), Phys. Rev. Lett. **115**, 222501 (2015).

[5] T. R. Saito *et al.*, Nucl. Phys. A **881**, 218 (2012).

[6] C. Rappold *et al.* (HypHI Collaboration), Phys. Rev. C **88**, 041001(R) (2013).

[7] C. Rappold *et al.*, Phys. Lett. B **747**, 129 (2015).

[8] Y. Zhu (STAR Collaboration), Nucl. Phys. A **904–905**, 551c (2013).

[9] J. Adam *et al.* (ALICE Collaboration), Phys. Lett. B **754**, 360 (2016).

[10] A. Esser, S. Nagao, F. Schulz, P. Achenbach *et al.* (A1 Collaboration), Phys. Rev. Lett. **114**, 232501 (2015).

[11] F. Schulz, P. Achenbach *et al.* (A1 Collaboration), Nucl. Phys. A **954**, 149 (2016).

[12] T. Miyoshi *et al.* (HNSS Collaboration), Phys. Rev. Lett. **90**, 232502 (2003).

[13] L. Yuan *et al.* (HNSS Collaboration), Phys. Rev. C **73**, 044607 (2006).

[14] M. Iodice *et al.* (Jefferson Lab Hall A Collaboration), Phys. Rev. Lett. **99**, 052501 (2007).

[15] F. Cusanno *et al.* (Jefferson Lab Hall A Collaboration), Phys. Rev. Lett. **103**, 202501 (2009).

[16] O. Hashimoto *et al.*, Nucl. Phys. A **835**, 121 (2010).

[17] F. Cusanno *et al.*, Nucl. Phys. A **835**, 129 (2010).

[18] S. N. Nakamura, A. Matsumura. Y. Okayasu, T. Seva, V. M. Rodriguez, P. Baturin *et al.* (HKS (JLab E01-011) Collaboration), Phys. Rev. Lett. **110**, 012502 (2013).

[19] L. Tang, C. Chen, T. Gogami, D. Kawama, Y. Han *et al.* (HKS (JLab E05-115 and E01-011) Collaborations), Phys. Rev. C **90**, 034320 (2014).

[20] G. M. Urciuoli *et al.* (Jefferson Lab Hall A Collaboration), Phys. Rev. C **91**, 034308 (2015).

[21] T. Gogami, C. Chen, D. Kawama *et al.* (HKS (JLab E05-115) Collaboration), Phys. Rev. C **93**, 034314 (2016).

[22] J. H. E. Mattauch, W. Thiele, and A. H. Wapstra, Nucl. Phys. **67**, 1 (1965).

[23] R. A. Brandenburg, S. A. Coon, and P. U. Sauer, Nucl. Phys. A **294**, 305 (1978).

[24] D. H. Davis, Nucl. Phys. A **754**, 3c (2005).

[25] R. H. Dalitz and F. Von Hippel, Phys. Lett. **10**, 153 (1964).

[26] J. L. Friar and B. F. Gibson, Phys. Rev. C **18**, 908 (1978).

[27] A. R. Bodmer and Q. N. Usmani, Phys. Rev. C **31**, 1400 (1985).

[28] M. Bedjidian *et al.*, Phys. Lett. B **62**, 467 (1976).

[29] M. Bedjidian *et al.*, Phys. Lett. B **83**, 252 (1979).

[30] A. Kawachi, Ph.D. thesis, University of Tokyo, Tokyo, Japan, 1997.

[31] A. Gal, Phys. Lett. B **744**, 352 (2015).

[32] D. Gazda and A. Gal, Phys. Rev. Lett. **116**, 122501 (2016).

[33] D. Gazda and A. Gal, Nucl. Phys. A **954**, 161 (2016).

[34] A. Gal, E. V. Hungerford, and D. J. Millener, Rev. Mod. Phys. (to be published), arXiv:1605.00557.

[35] T. Gogami, Ph.D. thesis, Tohoku University, Sendai, Japan, 2014.

[36] M. Jurič *et al.*, Nucl. Phys. B **52**, 1 (1973).

[37] H. Tamura *et al.*, Phys. Rev. Lett. **84**, 5963 (2000).

[38] D. R. Tilley, C. M. Cheves, J. L. Godwin, G. M. Hale, H. M. Hofmann, J. H. Kelley, C. G. Sheu, and H. R. Weller, Nucl. Phys. A **708**, 3 (2002).

[39] E. Hiyama, Y. Yamamoto, T. Motoba, and M. Kamimura, Phys. Rev. C **80**, 054321 (2009).

[40] O. Richter, M. Sotona and J. Žofka, Phys. Rev. C **43**, 2753 (1991).

[41] E. Hiyama, M. Isaka, M. Kamimura, T. Myo, and T. Motoba, Phys. Rev. C **91**, 054316 (2015).

[42] J. Pniewski and M. Danysz, Phys. Lett. **1**, 142 (1962).

[43] R. H. Dalitz and A. Gal, Nucl. Phys. B **1**, 1 (1967).

[44] J. Pniewski and Z. Szymański, D. H. Davis, and J. Sacton, Nucl. Phys. B **2**, 317 (1967).

[45] M. Sotona and S. Frullani, Prog. Theor. Phys. Suppl. **117**, 151 (1994).

[46] E. V. Hungerford, Prog. Theor. Phys. Suppl. **117**, 135 (1994).

[47] G. Xu and E. V. Hungerford, Nucl. Instrum. Methods Phys. Res. A **501**, 602 (2003).

[48] T. Gogami *et al.*, Nucl. Instrum. Methods Phys. Res. A **729**, 816 (2013).

[49] Y. Fujii *et al.*, Nucl. Instrum. Methods Phys. Res. A **795**, 351 (2015).

[50] G. Audi, A. H. Wapstra, and C. Thibault, Nucl. Phys. A **729**, 337 (2003).

[51] E. Hiyama and Y. Yamamoto, Prog. Theor. Phys. **128**, 105 (2012).

[52] E. Hiyama, Nucl. Phys. A **914**, 130 (2013).

[53] X. Mougeot *et al.*, Phys. Lett. B **718**, 441 (2012).